




Research Article

Microscopic Response of Limestone Physical Deterioration under Water-Rock Alternation in the Acidic Environment

Wei Liang ¹, Ke Li ^{1,2}, Jiashun Luo,³ Mengtang Xu ¹ and Fushou Feng¹

¹Institute of Mining Engineering, Guizhou Institute of Technology, Guiyang, Guizhou 550003, China

²School of Resource & Environment and Safety Engineering, Hunan University of Science and Technology, Xiangtan, Hunan 411201, China

³Institute of Subsurface Energy Systems, Clausthal University of Technology, Clausthal-Zellerfeld 38678, Germany

Correspondence should be addressed to Wei Liang; 20160713@git.edu.cn

Received 13 June 2022; Revised 21 July 2022; Accepted 27 July 2022; Published 22 August 2022

Academic Editor: Jim Shiau

Copyright © 2022 Wei Liang et al. This is an open access article distributed under the Creative Commons Attribution License, which permits unrestricted use, distribution, and reproduction in any medium, provided the original work is properly cited.

In order to investigate the microscopic response mechanism of limestone deterioration under alternating water-rock action in the acidic environment, the porosity, water absorption, mass loss characteristic, and microcrack propagation characteristic were analyzed by laboratory wetting-drying cyclic tests. The results show that, with increasing the number of cycles, the porosity, water absorption, and mass deterioration of the limestone specimens showed an overall increasing trend; moreover, at the beginning of the cycles, the physical deterioration of the specimen was significantly affected by the wetting-drying cycles, and at the end of the cycles, the physical deterioration of the specimen tended to be stable. The porosity deterioration degree reached 30.324% at the beginning of the cycles; there is a slight fluctuation in 20 cycles and then decreases as the number of cycles increases. The growth rate of water absorption increases slowly in 5~15 cycles and reaches the peak value in 20 cycles, and the growth rate decreases rapidly in the latter stages of the cycles. The increase rate of mass deterioration degree decreases with the increase of cycle number, the maximum average value can reach 61.887% at the beginning of cycles and is relatively stable at 20~25 cycles, and the average value at the end of cycle is obviously reduced by 3.167%. The nuclear magnetic resonance (NMR) test shows that the number and size of pores in the rock gradually increase with the increase of the number of wetting-drying cycles, and the wetting-drying cycles aggravate the internal damage of the rock. The number of shear cracks and fragmentation of the specimens increase as the increase of the number of cycles, and the failure of the specimens is mainly in the form of shear damage in the uniaxial compression test.

1. Introduction

The alternating wetting-drying cycles of rock are common in underground engineering field. The water-rock interaction weakens the physical and mechanical characteristics of the rock due to the presence of many microscopic or macroscopic crack defects in the rock itself [1], which leads to the deformation of the surrounding rock of underground engineering, roof caving, and other disasters. Many studies have been carried out about water-rock interaction. Yao et al. [2], Li et al. [3], Hu et al. [4], and Deng et al. [5] investigated the microstructure and mechanical properties of sandstone under water-rock interaction (wetting-drying cycles), and the results showed that water-rock interaction

has an effect of dissolution on the internal cement of sandstone, which leads to a significant deterioration effect on the microstructure and macroscopic strength properties. The experiments carried out by Tang revealed that water-rock interactions significantly decrease the shear strength of rock fractures [6]. For the rock damage effects in an acidic environment, Ding and Feng [7–9] analyzed the damaging effect of the microstructure of the rock and the fracture criterion of the fractured rock under chemical corrosion conditions and established the calculation formula of the damage variable based on the porosity. Through the analysis of the complete stress-strain curve of the triaxial compression test, the influence law of limestone deformation and strength corrosion effect is obtained. He and Guo [10] observed the

failure characteristics of the internal structure of the core under the action of acid by scanning electron microscope and analyzed the influence mechanism of different acid on the deformation characteristics and strength properties of limestone combined with the triaxial mechanical test. Huang et al. [11] considered that acidity had a significant influence on the characteristic parameters of red sandstones, such as surface features, mass and longitudinal wave velocity, porosity, thermal conductivity, and tensile strength. Li et al. [12] performed mechanical experiments on limestone to investigate the effects of different pH values of chemical solutions on porosity, microdamage, and macromechanical property deterioration. The pH values of the chemical solutions change the porosity and microdamage of the rock, which is the root cause of its mechanical property deterioration. According to Huang et al. [13], the acid solution causes sandstone to corrode and soften. The dynamic peak stress of sandstone is greatly affected by the acid dry-wet cycle, and as the pH of the acidic solution decreases, the elastic modulus and dynamic peak stress both decrease while the peak strain increases. Sandstone fragments exhibit more fractured blocks and smaller particle sizes as the acid dry-wet cycle intensifies. Nuclear magnetic resonance (NMR) technology was used by Wang [14], Zhao et al. [15], Zhong et al. [16], and Song et al. [17] to analyze the change law of microscopic pores of rock internal structure under water-rock action and then studied the influence law of rock microstructure deterioration on mechanical strength property damage. Liu et al. [18–20] studied the evolution law of microscopic pore deterioration in rocks under the action of wetting-drying cycles and discussed the effect of the number of wetting-drying cycles on the damage of rock strength parameters through mechanical experiments. With the help of discrete element software, the contact network, force chain distribution, and crack development law of particles inside the rock are analyzed. From the above analysis, it can be seen that under the physical and chemical action of the wetting-drying cycles, the rock microstructure changes continuously, such as the increase of primary pores or the generation of new microcracks that connect with each other; as a result, the macroscopic mechanical strength of the rock is greatly reduced.

Guizhou province is in the southwestern part of China with the most widely distributed karst landforms and in which the lithology is mainly limestone. Mastering rock mechanical properties is one of the essential theoretical foundations for mining engineering roadway support, roof control, and underground pressure management. From the above analysis, there are relatively few studies on the physical property deterioration of karst limestone in the Guizhou area under the action of alternating water-rock cycles in the acidic environment. Moreover, most of the predecessors primarily focused on the mechanical properties of sandstone, mudstone, and shale under the action of wetting-drying cycles, whereas in the microresponse of rock damage, only a single NMR technique or numerical simulation is usually considered, and the two are rarely analyzed combined. Based on the previous work, the wetting-drying cyclic experiments of limestone are carried out, and by combining NMR tech-

nology and numerical simulation in this study, the microresponse mechanism of limestone physical damage under the action of water-rock cycles in the acidic environment is discussed, and this establishes the foundation for follow-up research on the deterioration of limestone mechanical properties under the action of wetting-drying cycles.

2. Test Method

The specimens in this study are limestones with typical karst landforms in Guizhou province, which are gray, gray-black, and dense in structure. According to mineralogical analysis, the main minerals are 76.4% calcite, 21.2% dolomite, 1% quartz, less than 1% argillaceous, and other components less than 1%. The rock samples were processed into standard specimens with a diameter of 50 mm and a length of 100 mm. The specimens were soaked in an acidic solution with a pH of 2~4 for the wetting-drying cyclic test. The specimens were first naturally saturated in an acidic solution for 48 hours and then dried at 105°C for 24 hours, which is defined as a cycle. The experimental process is shown in Figure 1. The tests were carried out for 5, 10, 15, 20, 25, and 30 cycles. After each cycle was completed, the water absorption and mass of the specimens were tested, respectively, and the porosity test was carried out by NMR. The definition of deterioration degree in this work is described in the following equation:

$$D = \frac{|D_n - D_0|}{D_0} \times 100\%, \quad (1)$$

where D is the deterioration degree of the physical characteristic parameters after a certain cycle, D_n is the physical characteristic parameter of the specimens after a certain cycle, and D_0 is the physical characteristic parameter in the initial state.

To decrease the discreteness of the test data and avoid the impact of changes in the microstructure of the rock specimens on the test findings, the longitudinal wave velocity and natural density of specimens were conducted to test. The longitudinal wave velocity of the specimens can be conveniently measured by RSM-SY5(T) (see Figure 1), and the specimens with similar longitudinal wave velocity and natural density were selected for the wetting-drying cycle test. The specimens were separated into six groups, with two specimens in each group designated SY1 and SY2, respectively. The longitudinal wave velocity and natural density of specimens are shown in Table 1.

3. Test Result Analysis

3.1. Pore Deterioration Analysis. The porosity of rock is an important indicator to characterize the development degree of rock fractures, and it also indirectly reflects the internal structural characteristics of rocks. Its intricate micro and macropore structure controls the mechanical damage and deformation failure of rock [21]. The deterioration of rock microstructure in an acidic environment is primarily expressed in the changing of rock porosity due to the action

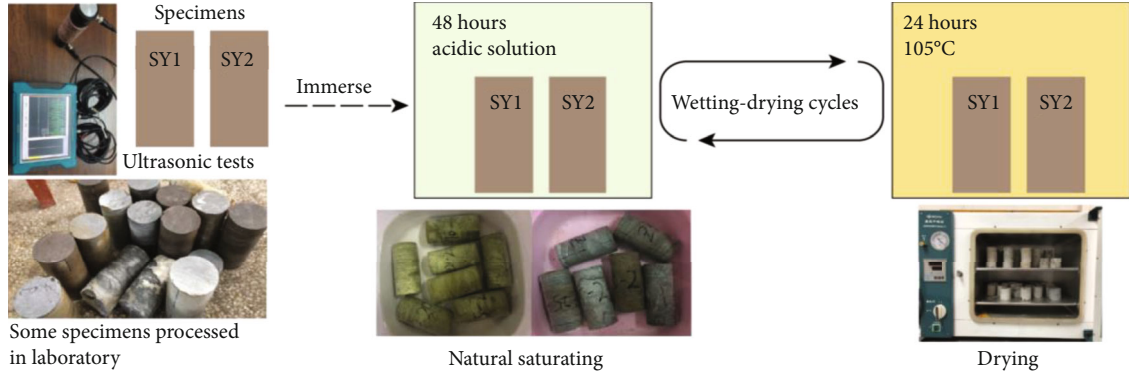


FIGURE 1: The process of the wetting-drying cyclic test.

TABLE 1: Longitudinal wave velocity and natural density of specimens.

Group No.	Longitudinal wave velocity (m/s)		Natural density (g/cm ³)	
	SY1	SY2	SY1	SY2
1	3620.045	3636.552	2.671	2.660
2	3796.221	3776.398	2.677	2.662
3	3707.845	3694.265	2.672	2.694
4	3860.323	3841.968	2.692	2.675
5	3663.455	3646.484	2.678	2.644
6	3903.520	3881.445	2.698	2.691
Average value	3752.377		2.676	

of wetting-drying cycles; the effective porosity of rock increases with increasing the number of cycles [22]. The porosity of rock specimens was determined by nuclear magnetic resonance (NMR) technology after wetting-drying cycles. The porosity and the degree of deterioration compared to the previous cycle are presented in Figure 2.

It can be seen from Figure 2 that with the increase of the number of cycles, the porosity of the specimens shows an increasing trend, and near the conclusion of the cycle (the number of cycles is 25-30), the porosity tends to be stable. The degree of pore deterioration is particularly high at the beginning of the cycle (the number of cycles is 5), with an average of 30.324%, and then gradually decreases. However, as the number of cycles reaches 20, the pore deterioration degree swings substantially, indicating an upward trend, and then reduces as the number of cycles increases overall.

3.2. Water Absorption Characteristic Analysis. The water absorption characteristic of rocks is one of the most significant indicators for evaluating the physical qualities of rocks as they represent the degree of development of pore structure and microcracks in the rock. The water absorption of the limestone specimens is obtained from the following equation [23, 24]:

$$\omega_{sa} = \frac{m_{sa} - m_{dr}}{m_{dr}} \times 100\%, \quad (2)$$

where m_{sa} represents the mass of a saturated specimen and m_{dr} is the mass of a dry specimen. The water absorption of rock under various cycles is shown in Figure 3.

Figure 3 demonstrates that the water absorption of the rock increases with the increase of the number of cycles and tends to be stable when it reaches 25-30 cycles. Compared with the growth rate of the previous cycle, the growth rate of rock water absorption is relatively steady in 5-15 cycles. When the number of cycles reaches 20, the growth rate of rock water absorption increases suddenly and then swiftly falls.

3.3. Mass Loss Analysis. The physical and chemical effects of rock minerals lead to rock disintegration and mineral dissolution under the conditions of wetting-drying cycles in an acidic environment, which results in the mass loss of rock. Mass loss is defined as the difference between the mass of the specimen after cyclic drying and the mass of the dry specimen in its natural state. Figure 4 presents the general variation trend of mass loss as it increases with the number of cycles. The mass loss of the specimens is gradually weakened by the number of cycles. When the number of cycles is 25~30, the mass loss degree is expected to steady.

In addition, the deterioration of the specimen mass is mainly owing to the mass loss caused by the dissolution of minerals in the acidic solution. The growth rate of the mass deterioration degree is relatively high in the early stage of the cycle, and the average maximum can reach 61.887%. However, the growth rate of mass loss degree reduces as the number of cycles increases and is relatively stable at 20-25 cycles, after which the growth rate of mass deterioration falls dramatically, with an average value of 3.167%, indicating that the speed of mass deterioration tends to decrease with the number of cycles. These results are in agreement with those obtained by D. T. Nicholson and F. H. Nicholson [25].

3.4. NMR Microstructure Damage Test. The nuclear magnetic resonance (NMR) technology uses the nuclear magnetic effect of hydrogen nuclei under the action of an external magnetic field. Pulses quantify the relaxation time of hydrogen nuclei in saturated rock specimens, reflecting the pore size and fraction of the pores in the rock specimen [17, 26]. The value of the relaxation time on the horizontal

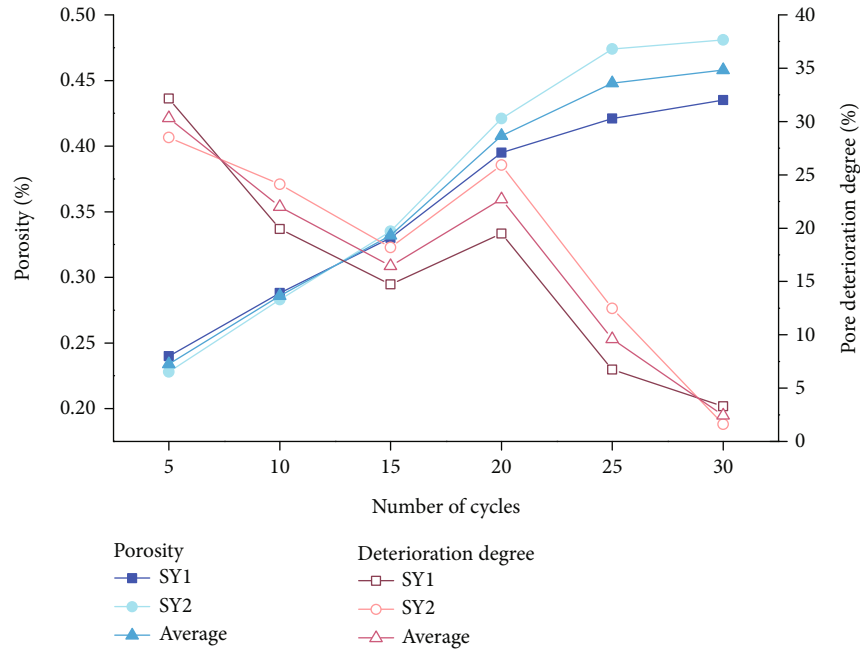


FIGURE 2: The variation law of porosity and deterioration degree.

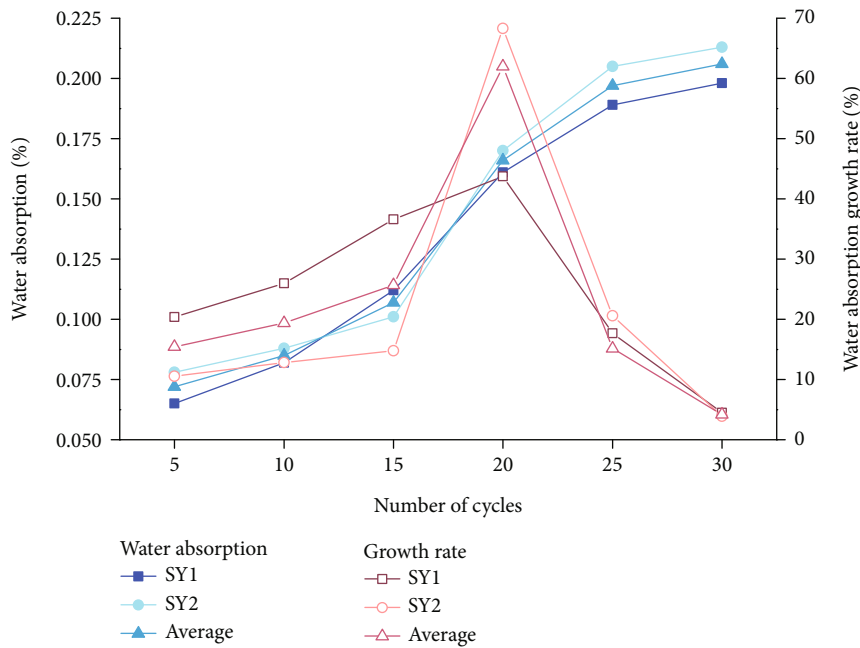


FIGURE 3: The variation law of water absorption.

axis (T_2) is proportional to the pore size distribution, that is, the horizontal axis indicates that the pore size gradually increases from left to right. The amplitude of the signal on the vertical axis is proportional to the proportion of pores, and its peak value represents the fraction of pores corresponding to the pore size [17, 26].

The T_2 chart of different wetting-drying cycles, shown in Figure 5, has three peak regions corresponding to micropores, mesopores, and macropores from left to right. The cumulative value of the signal (spectral peak area) represents

the proportion of pores in a certain pore size range. The figure shows that the rock specimens are mainly composed of micropores and mesopores, while the proportion of macropores is not obvious. However, with the increase of the number of wetting-drying cycles, the peak value of the T_2 curve and the span of the horizontal axis gradually increase, indicating that as the number of cycles increases, the number of pores and pore size in the rock gradually increase as well. In other words, the wetting-drying cycles aggravate the microstructural deterioration inside the rock.

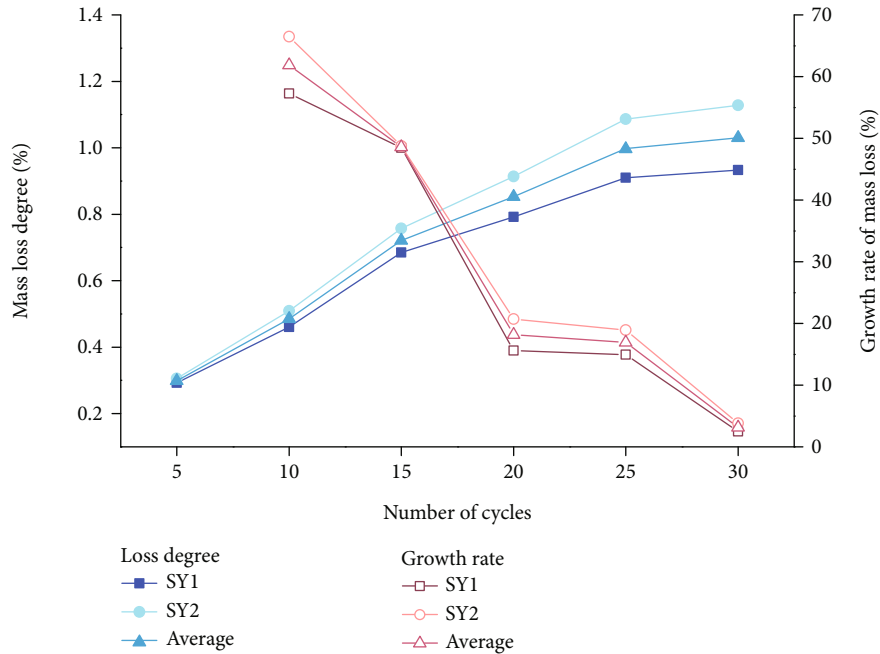


FIGURE 4: The variation of mass loss.

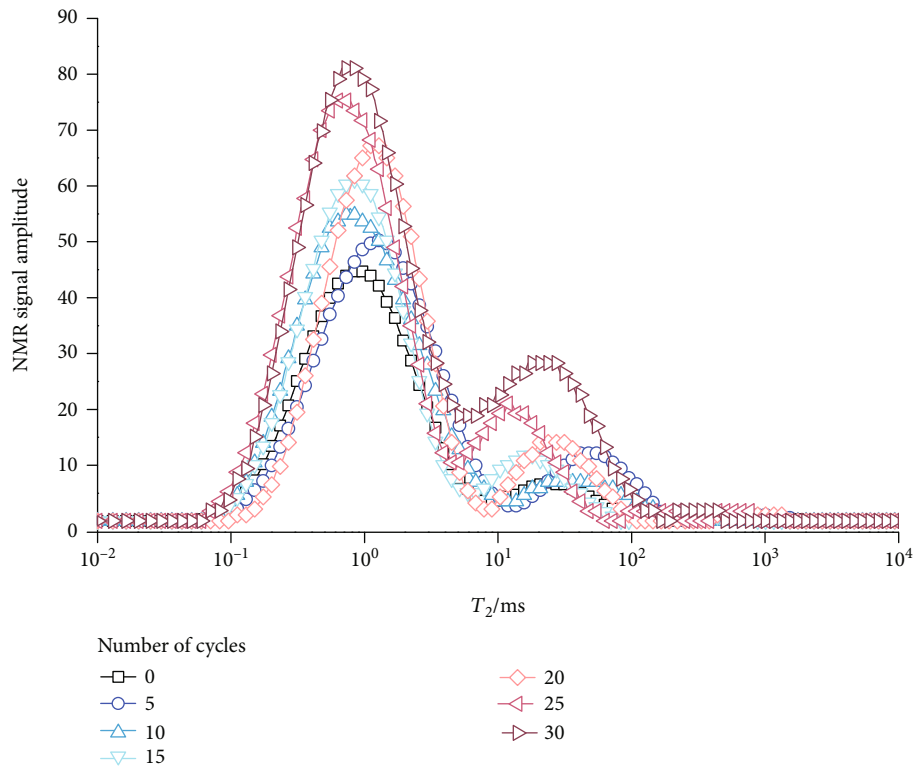


FIGURE 5: The T_2 curves of different wetting-drying cycles.

4. Numerical Analysis of Microcrack Propagation in Uniaxial Compression

The discrete element method (DEM) has been widely used in the microscopic study of rock mechanics [27–30]. The particle flow code (PFC) is a numerical method based on

the DEM that represents the rock as a dense packing of nonuniform-sized cemented particles bonded together at their contact points and whose mechanical behavior is defined by the bonded-particle model [27, 31]. This method is useful for investigating the mechanical properties of rock during wetting-drying cycles [32–34]. In this study, a

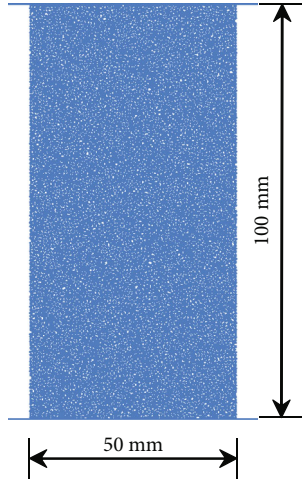


FIGURE 6: PFC numerical model.

numerical simulation of microcrack propagation in uniaxial compression was performed using PFC. The size of the PFC model specimen is 50 mm in diameter and 100 mm in length, as shown in Figure 6. It is necessary to take into account the REC in the modeling because it is an important parameter to determine the particle size of the model. Previous studies have shown that when the REC is greater than 10, the effect of particle size on the simulation results of the model is negligible [33, 35, 36]. The REC is defined as follows:

$$\text{REC} = \left(\frac{L}{R_{\min}} \right) \left[\frac{1}{(1 + R_{\max}/R_{\min})} \right], \quad (3)$$

where L is the minimum size of the specimen, R_{\min} is the minimum particle size, and R_{\max} is the maximum particle size. According to Castro-Filgueira et al. and Potyondy and Cundall [27, 31], the R_{\max}/R_{\min} value of 1.66 is the best for reproducing a rock specimen, and the model satisfies the requirement when the value of R_{\min} is 0.3 mm. Furthermore, the stress-strain curve of the uniaxial compression test derived using the flat-joint contact model can adequately represent rock mechanical properties [27, 31, 37].

The microscopic crack propagation and structural fragmentation distribution features of the specimens under the action of uniaxial compressive are analyzed in this study, as well as the microresponse of limestone deterioration under the action of wetting-drying cycles. The uniaxial compressive stress-strain curve is shown in Figure 7.

Figure 7 illustrates that with the increase of the number of wetting-drying cycles, the peak strength of the rock sequentially decreases, as does the slope of the stress-strain curve. Other researchers' findings have revealed a similar tendency [19, 38]. The numerical simulation findings reveal that the peak strength of the rock for cycles 5, 15, and 30 is reduced by 19.81%, 17.75%, and 28.03%, respectively, compared with the previous stage cycle. The numerical simulation findings are generally consistent with the results

obtained from the laboratory experiments, which can be used as a basis for subsequent analysis.

Figure 8 shows the specimen's microscopic fracture development and fragmentation distribution following uniaxial compression failure. Generally, the specimen is mainly damaged along the direction of the shear crack. In the natural state (in the case with 0 cycle), the microcracks show a development trend of obliquely penetrating from the top to the bottom of the specimen, and the degree of fragmentation is low, indicating that the damaged block is mainly intact. After five cycles, the shear microcrack had completely penetrated the top and bottom of the specimen, and the fragmentation along the shear failure surface had gradually increased. After 15 cycles, the number of shear cracks rose and rapidly spread to the side of the specimen, eventually breaking it. After 30 cycles, the shear crack developed to the ends and sides of the specimen, the fragmentation of the specimen increased significantly, and many tiny rock blocks were created when the specimen was broken. The failure characteristics of the specimens mentioned above are consistent with the results of laboratory experiments. In a word, with the increase in the number of drying and wetting cycles, the number of shear cracks and fragmentation gradually increases, and the failure mode of the specimens is mainly manifested as shear failure.

5. Discussion

According to the test results, the wetting-drying cycle has a significant impact on the physical properties of limestone specimens such as porosity, water absorption, and mass. Figure 9 demonstrates the change in appearance of some specimens after cyclic immersion. After soaking in the acidic solution, the mineral particles, initial defects (such as cracks), and roughness of the specimen's surface become more visible, indicating that the physical and chemical reaction occurred between the specimen and the solution, and the structural integrity of the specimen was eroded. In particular, the specimens with initial defects and coarse mineral particles have more obvious erosion traces, and the more cycles, the stronger the erosion effect.

It can be seen from the relationship between the porosity and deterioration of the aforementioned specimens that the average porosity of the specimen increased from 0.179% in the initial (0 cycle) to 0.458% in 30 cycles, an overall increase of 155.87%. The degree of deterioration reached its maximum at the beginning of cycles, with an average value of 30.324%, and then, there is a fluctuation point at 20 cycles, after which it drops to 2.452% at the end of the cycles, which shows that the porosity presents a nonlinear variation law with the number of wetting-drying cycles, and it is because the limestone mineral components are more sensitive to the wetting-drying cycles in an acidic environment. Calcite, the primary mineral in limestone, chemically interacts with acid ions in the solution, destroying the bonding between mineral particles or crystals and causing changes in their microstructure. The deterioration process can be described as the chemical reaction caused by water infiltrating into the rock through the primary microcracks, resulting in the

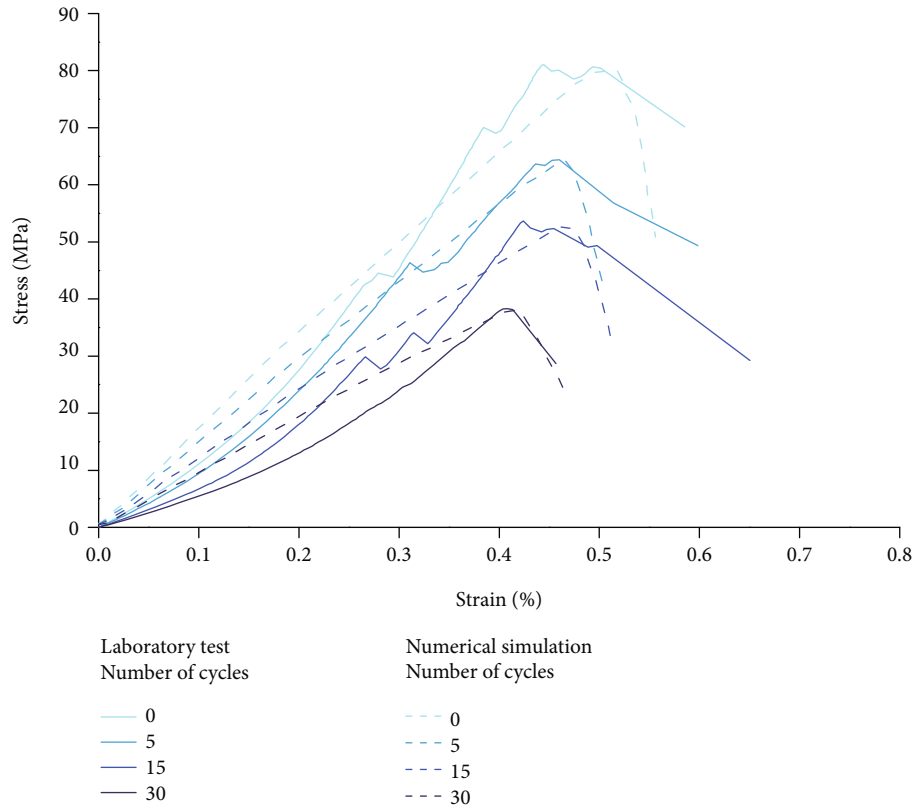


FIGURE 7: Stress-strain curve of uniaxial compression test.

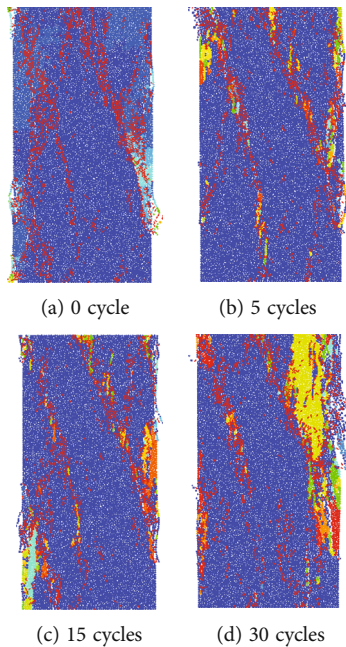


FIGURE 8: Microcrack propagation under different cycle conditions.

dissolution of minerals and the expansion of microcracks and primary cracks, as well as increasing the specimen's porosity [39]. The test findings show that porosity increases steadily over 5~15 cycles while the degree of deterioration decreases as compared to the preceding cycle, which indi-

cates that the minerals in the specimen were progressively dissolved to produce micropores at this stage, but the rate of pores develops slowly. When the number of cycles is increased to 20, the degree of pore deterioration dramatically increases, indicating that the microscopic cracks of the



FIGURE 9: Change of appearance characteristics of some specimens after cyclic immersion.

specimen are interconnected or the primary cracks expand, resulting in a significant increase in porosity. Moreover, the presence of minerals or chemical reactants are difficult to completely dissolve, which slows the rate of physical and chemical reactions. Therefore, in the postcycle period, the porosity growth slows down and the deterioration degree decreases. It can be seen from the T_2 curves that the increase in specimen porosity is mainly dominated by micropores and mesopores, which is caused by the dissolution of soluble minerals in the specimens to generate new micropores. Then, the micropores gradually transform into mesopores as the number of cycles increases. However, with the reduction of soluble minerals, the continuous deterioration of pores is diminished, and the internal damage of the specimen gradually tends to be stable in the later period of drying and wetting cycles [17].

The variation in the water absorption characteristics of the specimens indicates that as the number of cycles increases, the average water absorption rate increases from 0.072% to 0.206%, and the average water absorption growth rate reaches a peak value of 61.974% at 20 cycles; then, it drops to 4.202% and levels off at the end of the experiment. The water absorption process of rock is not that the rock mineral particles themselves absorb water, but the water occupies the micro or macropores between the particles. Therefore, the change in water absorption is mainly determined by the characteristics of the pores within the rock and its changing law [33]. The test results show that the water absorption rate of rock has a similar relationship to the aforementioned pore deterioration process, in that it increases relatively smoothly in the early stage of the cycle, suddenly increases after 20 cycles, and then decreases significantly and tends to be stable in the later period.

From the numerical simulation results of uniaxial compression, enhancing the number of drying and wetting cycles, the deterioration of the microporous structure inside the specimen destroys structural integrity and reduces the bonding strength of microscopic particles; as a result, the

number of microcracks gradually increases and penetrates both ends of the specimen under the load. Meanwhile, the fragmentation along the crack surface gradually increases and develops towards the end and side of the specimen, and the microscopic particle contact fracture is intensified, which is reflected in the macroscopically shearing failure and the formation of more fragments.

The foregoing research also shows that indexes such as rock porosity, water absorption, and mass are the parameters that describe the physical properties of rock specimens, the essence of the damage is that the rock specimen is eroded by acid, which leads to the deterioration of the internal structure and the expansion of primary fractures, and the initial wetting-drying cycle has a great influence on the physical deterioration of the specimen. The influencing factors of physical damage of limestone under dry-wet cycle conditions are mainly reflected in aspects of macroscopic and microscopic, the presence of macroscopic crack initiation defects provides an erosion path for the acidic solution, and when the solution penetrates the internal structure of the rock, it leads to the generation of microscopic pores, which aggravates the comprehensive deterioration effect to the rock.

6. Conclusion

- (1) The degree of pore degeneration compared to the previous cycle is relatively high, with an average of 30.324% at the beginning of the cycle and then gradually decreasing. However, the degree of pore deterioration showed an increasing trend at 20 cycles and then decreased overall with the increase of the number of cycles
- (2) The water absorption rate of the rock increases with the increase in the number of cycles and tends to be stable when it reaches 25-30 cycles. The growth rate of rock water absorption is relatively steady at 5-15 cycles. The average water absorption growth rate

reaches a peak value of 61.974% at 20 cycles and then decreases rapidly in the later period of cycles

- (3) The growth rate of mass loss degree reduces as the number of cycles increases. It is relatively high in the early stages of the cycles, and the average maximum reaches 61.887% and is relatively stable at 20–25 cycles, after which the growth rate of mass loss falls dramatically, with an average value of 3.167%
- (4) With the increase of the number of wetting-drying cycles, the peak value of the T_2 curve and the horizontal axis's span gradually increase, indicating that the number of pores and pore diameter gradually increase, and wetting-drying cycles aggravate the microstructural deterioration within the rock
- (5) With the increase of the number of drying and wetting cycles, the number of shear cracks and fragmentation gradually increases under uniaxial compression, and the failure of the specimens is mainly with a shear failure mode

Data Availability

The data used to support the findings of this study are included within the article.

Conflicts of Interest

All the authors declare that they have no known conflicts of interest that could influence the work reported in this paper.

Acknowledgments

The work described in this paper has received financial support from the Guizhou Provincial Science and Technology Projects (No. QKHZC [2021] General 407), the New Talent Training Project of Guizhou Institute of Technology (No. GZLZX-29), the National Natural Science Foundation of China (No. 52104123), and the China Scholarship Council (No. 202108525011).

References

- [1] Z. D. Lu, *Experimental and Theoretical Analysis on Mechanical Properties of Fractured Rock under Water-Rock Interaction*, [Ph.D. thesis], Institute of rock & soil mechanics, Chinese academy of science, P.R. China. CNKI (2010238532), 2010.
- [2] H. Y. Yao, Z. H. Zhang, C. H. Zhu, Y. C. Shi, and Y. Li, "Experimental study of mechanical properties of sandstone under cyclic drying and wetting," *Rock and Soil Mechanics*, vol. 31, no. 12, pp. 3704–3708, 2010.
- [3] J. Li, L. H. Wang, Z. J. Chen, and L. Xiang, "Study on deterioration characteristics of sandstone under long-term immersion and dry-wet cycle," *Water Resources and Power*, vol. 35, no. 3, pp. 123–126, 2017.
- [4] Y. Hu, H. F. Deng, J. L. Li, Y. C. Zhang, W. Wang, and Y. Y. Hu, "Research on characteristics and mechanism of microstructure variation in sandstone under water-rock interaction," *Journal of Disaster Prevention and Mitigation Engineering*, vol. 38, no. 2, pp. 265–273, 2018.
- [5] H. F. Deng, Y. Y. Zhi, L. L. Duan, D. Pan, and J. L. Li, "Research on the mechanical properties of sandstone and the damage evolution of microstructure under water-rock interaction," *Rock and Soil Mechanics*, vol. 40, no. 9, pp. 3447–3456, 2019.
- [6] Z. C. Tang, Q. Z. Zhang, and Y. Zhang, "Cyclic drying-wetting effect on shear behaviors of red sandstone fracture," *Rock Mechanics and Rock Engineering*, vol. 54, no. 5, pp. 2595–2613, 2021.
- [7] W. X. Ding and X. T. Feng, "Testing study on mechanical effect for limestone under chemical erosion," *Chinese Journal of Rock Mechanics and Engineering*, vol. 23, no. 21, pp. 3571–3576, 2004.
- [8] W. X. Ding and X. T. Feng, "Damage effect and fracture criterion of rock with multi-preexisting cracks under chemical erosion," *Chinese Journal of Geotechnical Engineering*, vol. 31, no. 6, pp. 899–904, 2009.
- [9] W. X. Ding and X. T. Feng, "Study on chemical damage effect and quantitative analysis method of meso-structure of limestone," *Chinese Journal of Rock Mechanics and Engineering*, vol. 24, no. 8, pp. 1283–1288, 2005.
- [10] C. M. He and J. C. Guo, "Mechanism study of acid on mechanical properties of limestone," *Chinese Journal of Rock Mechanics and Engineering*, vol. 32, no. S2, pp. 3016–3021, 2013.
- [11] Z. Huang, W. Zeng, Y. Wu, S. Li, Q. Gu, and K. Zhao, "Effects of temperature and acid solution on the physical and tensile mechanical properties of red sandstones," *Environmental Science and Pollution Research International*, vol. 28, no. 16, pp. 20608–20623, 2021.
- [12] H. Li, Z. Zhong, X. Liu, Y. Sheng, and D. Yang, "Micro-damage evolution and macro-mechanical property degradation of limestone due to chemical effects," *International Journal of Rock Mechanics and Mining Sciences*, vol. 110, pp. 257–265, 2018.
- [13] X. Huang, J. Pang, and J. Zou, "Study on the effect of dry-wet cycles on dynamic mechanical properties of sandstone under sulfuric acid solution," *Rock Mechanics and Rock Engineering*, vol. 55, no. 3, pp. 1253–1269, 2022.
- [14] S. Wang, "Analysis of rock pore structural characteristic by nuclear magnetic resonance," *Xinjiang Petroleum Geology*, vol. 30, no. 6, pp. 768–770, 2009.
- [15] H. Zhao, L. Q. Sima, Q. B. Yan, and J. Y. Li, "NMR experiments and analysis of carbonate rock samples," *Well Logging Technology*, vol. 35, no. 2, pp. 117–121, 2011.
- [16] Z. L. Zhong, W. K. Luo, X. R. Liu, H. Li, J. Chen, and X. X. Hu, "Experimental study on mechanical properties deterioration of limestone in acid environment based on nuclear magnetic resonance," *Journal of China Coal Society*, vol. 42, no. 7, pp. 1740–1747, 2017.
- [17] Y. J. Song, L. T. Zhang, J. X. Ren et al., "Study on damage characteristics of weak cementation stratum under wetting-drying cycles based on nuclear magnetic resonance technique," *Chinese Journal of Rock Mechanics and Engineering*, vol. 38, no. 4, pp. 825–831, 2019.
- [18] X. R. Liu, W. Yuan, Y. Fu, Z. J. Wang, L. L. Miao, and W. B. Xie, "Porosity evolution of sandstone dissolution under wetting and drying cycles," *Chinese Journal of Geotechnical Engineering*, vol. 40, no. 3, pp. 527–532, 2018.
- [19] X. Liu, D. Li, Z. Wang, and L. Zhang, "Influence of wetting-drying cycles on mechanical properties and microstructure of shaly sandstone," *Chinese Journal of Geotechnical Engineering*, vol. 38, no. 7, pp. 1291–1300, 2016.

- [20] X. R. Liu, L. Zhang, and Y. Fu, "Experimental study of mechanical properties of argillaceous sandstone under wet and dry cycle in acid environment," *Rock and Soil Mechanics*, vol. 35, no. S2, pp. 45–52, 2014.
- [21] T. De Kock, M. A. Boone, T. De Schryver et al., "A pore-scale study of fracture dynamics in rock using X-ray micro-CT under ambient freeze–thaw cycling," *Environmental Science & Technology*, vol. 49, no. 5, pp. 2867–2874, 2015.
- [22] A. Dehestani, M. Hosseini, and A. T. Beydokhti, "Effect of wetting–drying cycles on mode I and mode II fracture toughness of sandstone in natural (pH=7) and acidic (pH=3) environments," *Theoretical and Applied Fracture Mechanics*, vol. 107, pp. 1025–1030, 2020.
- [23] Y. Zhang, Z. Wang, G. Su, Z. Wu, F. Liu, and M. Jingjing, "Experimental investigation on influence of acidic dry-wet cycles on karst limestone deterioration and damage," *Geofluids*, vol. 2022, Article ID 8562226, 12 pages, 2022.
- [24] S. Huang, J. Wang, Z. Qiu, and K. Kang, "Effects of cyclic wetting–drying conditions on elastic modulus and compressive strength of sandstone and mudstone," *Processes*, vol. 6, no. 12, pp. 234–249, 2018.
- [25] D. T. Nicholson and F. H. Nicholson, "Physical deterioration of sedimentary rocks subjected to experimental freeze–thaw weathering," *Earth Surface Processes and Landforms: The Journal of the British Geomorphological Research Group*, vol. 25, no. 12, pp. 1295–1307, 2000.
- [26] K. G. Li, B. W. Yang, and Q. C. Qin, "Experimental study on unloading damage and permeability of dolomite based on nuclear magnetic resonance technique," *Chinese Journal of Rock Mechanics and Engineering*, vol. 38, no. S2, pp. 3493–3502, 2019.
- [27] U. Castro-Filgueira, L. R. Alejano, and J. Arzúa, "Numerical simulation of the stress-strain behavior of intact granite specimens with particle flow code," in *ISRM International Symposium-EUROCK 2016*, London, 2016 Taylor & Francis Group.
- [28] O. K. Mahabadi, B. E. Cottrell, and G. Grasselli, "An example of realistic modelling of rock dynamics problems: FEM/DEM simulation of dynamic Brazilian test on Barre granite," *Rock Mechanics and Rock Engineering*, vol. 43, no. 6, pp. 707–716, 2010.
- [29] M. Nikolić, T. Roje-Bonacci, and A. Ibrahimbegović, "Overview of the numerical methods for the modelling of rock mechanics problems," *Tehnicki vjesnik - Technical Gazette*, vol. 23, no. 2, pp. 627–637, 2016.
- [30] S. Yang, P. Yin, and Y. Huang, "Experiment and discrete element modelling on strength, deformation and failure behaviour of shale under Brazilian compression," *Rock Mechanics and Rock Engineering*, vol. 52, no. 11, pp. 4339–4359, 2019.
- [31] D. O. Potyondy and P. A. Cundall, "A bonded-particle model for rock," *International Journal of Rock Mechanics and Mining Sciences*, vol. 41, no. 8, pp. 1329–1364, 2004.
- [32] X. Huang and J. Pang, "Study on the change of physical properties of sandstone under action of acidic drying–wetting cycles and discrete element simulation," *Bulletin of Engineering Geology and the Environment*, vol. 80, no. 10, pp. 7773–7790, 2021.
- [33] G. Wu, W. Chen, and K. Cui, "The numerical simulation of influence of drying–wetting cycles on the deterioration characteristics of gypsum rocks under particle flow code," *Earth Sciences Research Journal*, vol. 24, no. 1, pp. 55–59, 2020.
- [34] Z. Shi, J. Li, and Y. Zhao, "Study on damage evolution and constitutive model of sandstone under the coupled effects of wetting–drying cycles and cyclic loading," *Engineering Fracture Mechanics*, vol. 253, article 107883, 2021.
- [35] Z. H. Xu, W. Y. Wang, P. Lin, Y. Xiong, Z. Y. Liu, and S. J. He, "A parameter calibration method for PFC simulation: development and a case study of limestone," *Geomechanics and Engineering*, vol. 22, no. 1, pp. 97–108, 2020.
- [36] Y. Zhou, S. Wu, J. Jiao, and X. Zhang, "Research on mesomechanical parameters of rock and soil mass based on BP neural network," *Rock and Soil Mechanics*, vol. 32, no. 12, pp. 3821–3826, 2011.
- [37] U. Castro-Filgueira, L. R. Alejano, and D. M. Ivars, "Particle flow code simulation of intact and fissured granitic rock samples," *Journal of Rock Mechanics and Geotechnical Engineering*, vol. 12, no. 5, pp. 960–974, 2020.
- [38] S. Chen, T. Jiang, H. Wang, F. Feng, D. Yin, and X. Li, "Influence of cyclic wetting–drying on the mechanical strength characteristics of coal samples: a laboratory-scale study," *Energy Science & Engineering*, vol. 7, no. 6, pp. 3020–3037, 2019.
- [39] H. F. Deng, Z. Y. Xiao, J. L. Li, Y. Y. Hu, and M. L. Zhou, "Deteriorating change rule test research of damage sandstone strength under water–rock interaction," *Chinese Journal of Rock Mechanics and Engineering*, vol. 34, no. S1, pp. 2690–2697, 2015.